An Experiment in Model-Based Boundary Detection

PJ Azzopardi† D Pycock CJ Taylor AC Wareham‡

Wolfson Image Analysis Unit, Department of Medical Biophysics,
Department of Physiological Sciences,‡
University of Manchester, Manchester M13 9PT

This paper describes a simple model-based approach to boundary detection for blob *shaped objects. A geometric model is used to focus attention on relevant portions of the image during boundary generation. The boundary generated is that which is a globally optimal match to the shape and edge description parameters of the model. The method is illustrated using images of stained transverse sections of skeletal muscle and the adaptability of the model is demonstrated using images of cells of the corneal endothelium which have poor grey-level contrast.*

The task of image interpretation involves the combination of both low-level and high-level processes. Low-level processes, such as edge detection, are primarily numerical and deal directly with data in image arrays. High-level processes are more symbolic in nature and deal with abstracted image features. Models of expected image structure have been proposed as a means of providing a framework within which high-level and low-level processing can be integrated. However, a truly general approach has yet to be reported and many issues remain to be investigated.

One of the problems which arise from the use of models is the computational complexity of the matching process[11]. Even relatively simple model-matching tasks may be of sufficient complexity to strain the performance of any presently conceivable machine[10]. One way of coping with this problem is to use cues to focus attention on likely interpretations, thus avoiding computational effort being wasted on the more unlikely ones.

Cues can be thought of as evidence of structure which may be used in conjunction with models to generate hypotheses about the presence of other structures in the image. In the earliest stages of image interpretation it is probably inevitable that cue generation depends on the use of unguided low-level processes, but it is important to recognise that evidence gathered in this way is not likely to represent the best which could be sought in support of a particular emerging hypothesis. In practice, it may be necessary to use a strategy of successive refinement, in which unguided low-level processes can be used to provide sufficient evidence for an initial interpretation which may then be used as an organising hypothesis, to guide the collection and interpretation of further low-level evidence. This new evidence may in turn lead to yet further refinements of interpretation.

In this paper we describe some work in which we have attempted to explore the two key ideas of cue generation and successive refinement of interpretation by applying them to a practical problem. The example which we have chosen is the analysis of transverse sections of skeletal muscle fibres stained to show myosin ATPase activity as shown in Fig. 1. A common requirement in the analysis of such images is to measure the size, shape and density of stain uptake for a large number of fibres. To do this it is necessary to delineate fibre boundaries, a tedious and time consuming task to undertake manually.

Previous work[3, 5] has predominantly involved low-level processing and paid little attention to the formal representation of knowledge. Mc Queen[6] describes a model-based bubble-growing algorithm for finding the boundaries of fibres in preparations similar to those which we have used. He acknowledges, however, that this is a computationally expensive process. No attempt was made to reduce the computational load by using a focus of attention strategy; bubbles are initiated at arbitrary points in the image.

OVERVIEW OF THE METHOD

Skeletal muscle is composed of compact bundles of fibres which, when sectioned, stained and mounted, appear in cross-section as a pavement of distorted round objects (see Fig. 1). The design of the model used to detect the fibre boundaries was influenced by the observations that the fibres tend (i) to have visible edges, (ii) to be convex in shape and (iii) to be

This work was supported by the University of Manchester Research Support Fund.

† *Present address: Department of Experimental Psychology, University of Oxford.*

AVC 1988 doi:10.5244/C.2.6

separated from neighbouring fibres by gaps (caused by a slight shrinkage during preparation). The basis of the model is the idea that the boundary of a convex object can easily be reconstructed by joining points on a set of radial vectors which emanate from a point near its centre.

The task of detecting the fibre boundaries was broken down into three main steps:-

1. The generation of object centre cues
2. The generation of multiple boundary cues
3. The instantiation of the boundary

The knowledge used to detect the fibre boundaries is summarised in Table 1. This is organised according to four levels of abstraction, namely those of the raw image, the fibre centres, the boundary points and the boundaries. The abstraction of data between one level and the next is performed in a single cycle of cue generation and evidence gathering as an interpretation of the image is progressively refined.

CENTRE CUE GENERATION

The purpose in identifying object centre cues is to focus attention on those locations in the image where objects of interest are most likely to be found. The strategy adopted reflects the model of a mainly convex, *blob* shaped feature which is used to guide boundary detection. Centre cues are defined as the locus of points maximally distant from a boundary found in an approximate edge segmentation. This process is illustrated in Figs. 2-5. The original image of stained skeletal muscle fibres is shown in Fig. 1 The first step in the process is to generate a gradient map by taking the difference between the original image and its grey-level erosion. This and other morphological grey-level operators are described by Serra[9].

Next the bimodal separation of grey-levels in this edge map is enhanced using a non-linear grey-level relaxation algorithm[8] to first stretch the distribution of grey-level values in the image and in a second pass to cluster values around the nearest peak (light or dark) in a grey level distribution histogram of the transformed image. The result of this pre-processing is shown in Fig. 2.

The selection of a threshold to give an approximate segmentation of the relaxed edge image is not critical. The result of automatic thresholding is shown in Fig. 3. The apparent completeness of the edge segmentation is beguiling. We have investigated the use of both binary and grey-level opening and closing operations[10] but have found it impossible to complete the segmentation using them. This is, however, of no importance since the objective here is to obtain a reasonable approximation which is applicable over a broad range of conditions.

A distance transformation is applied to the results of the segmentation using a two-pass propagation algorithm[2] (Fig. 4). The peaks in this map are identified using a second, rapidly convergent, iterative, two-pass propagation algorithm. These peaks are maximally distant from the edges initially detected and their positions roughly correspond to the centres of the muscle fibres in the original image, as shown in Fig. 5. The peak positions are used as cues to initiate the search for fibre boundaries. The generation of more than one centre cue per cell, which sometimes occurs, does not pose a serious problem since the similarity of the boundaries subsequently instantiated can easily be recognised at a later stage.

Table 1. Summary of Knowledge Utilisation

Level of Abstraction	A priori Knowledge	Application of Knowledge	Influence on interpretation
A. Raw Image	Objects have edges	Edge map	Weak
B. Candidate objects	Centre of object distant from edges	Distance transform	Weak
C. Candidate boundary points	Radials cross boundary	Search radius	Absolute
	Edges perpendicular to radials	Directional edge detection	Weak
D. Candidate boundary	Boundary not re-entrant	Ordering of radials	Absolute
		One boundary point per radial selected	Absolute
	Objects are compact	Radial continuity	Weak
	Gaps next to boundaries	Top hat edge model	Weak

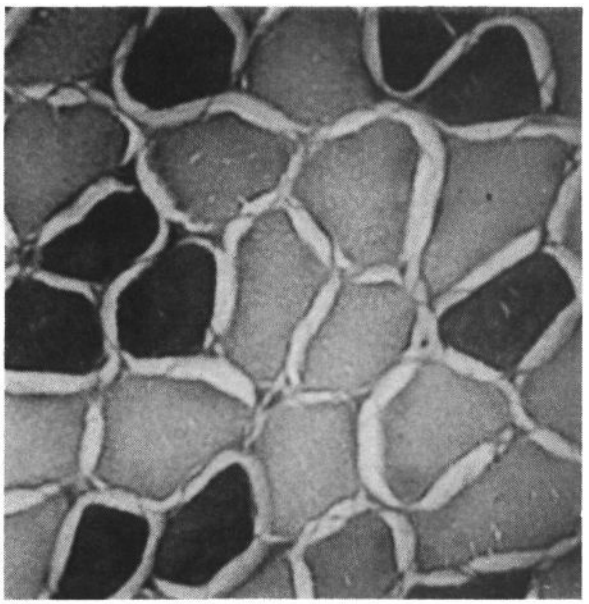

Figure 1. Image of stained section of skeletal muscle fibre.

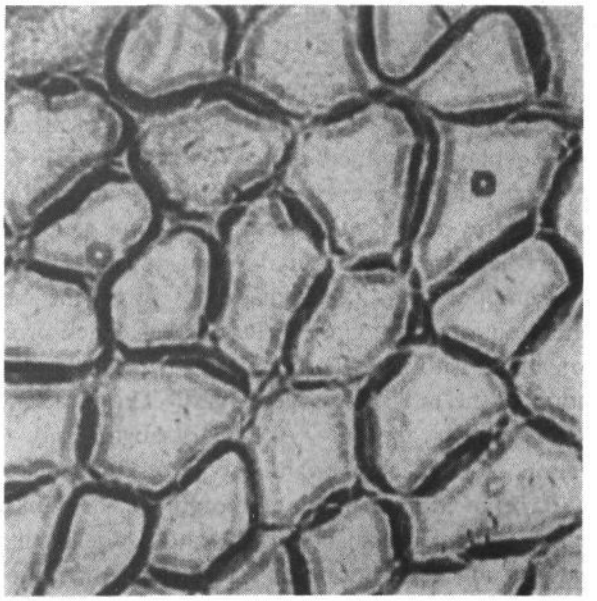

Figure 2. Grey-level image of edge strength from Fig. 1 after relaxation labelling.

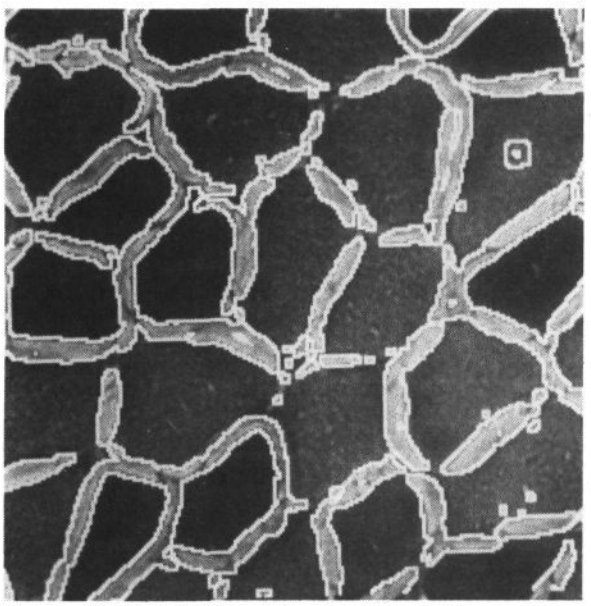

Figure 3. Initial boundary segmentation.

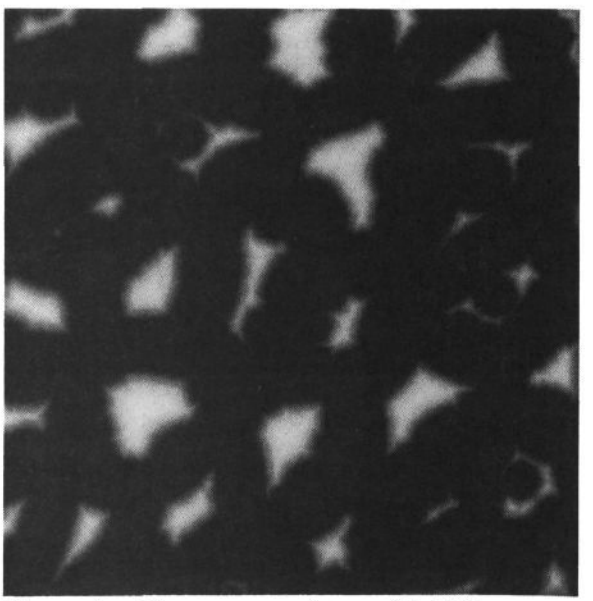

Figure 4. Distance transform of initial segmentation.

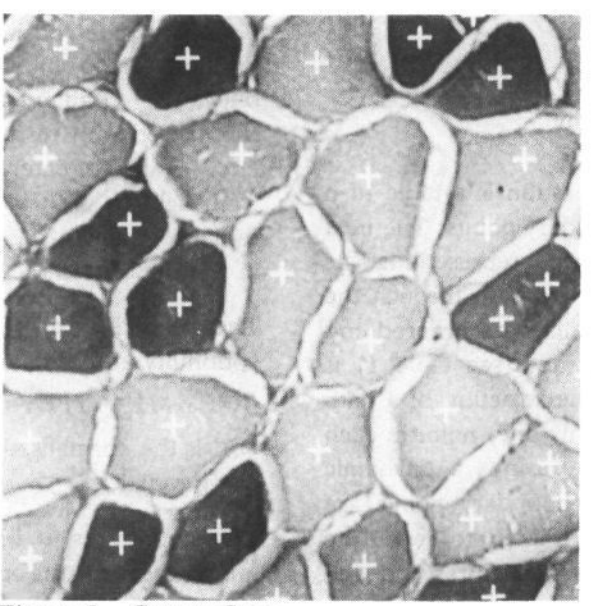

Figure 5. Centre Cues.

BOUNDARY CUE GENERATION

Boundary cues are generated by searching for the m most significant grey-level edges along a set of n radial profiles centered on each centre cue, as shown in Fig. 6. Each radial grey-level profile is formed by averaging grey-level values in a direction perpendicular to the radial path. This spatial averaging is justified on the assumption that the radial lines cross the fibre boundary at an angle close to 90 degrees. Each profile is convolved with a first order derivative filter and the location of the m largest edges found. The location of these edges, a measure of the strength and the direction of change in brightness across the edge (ie light-dark or dark-light) are stored for use in the selection of an optimal boundary path. The result of boundary cue generation for a single centre cue is shown in Fig 7.

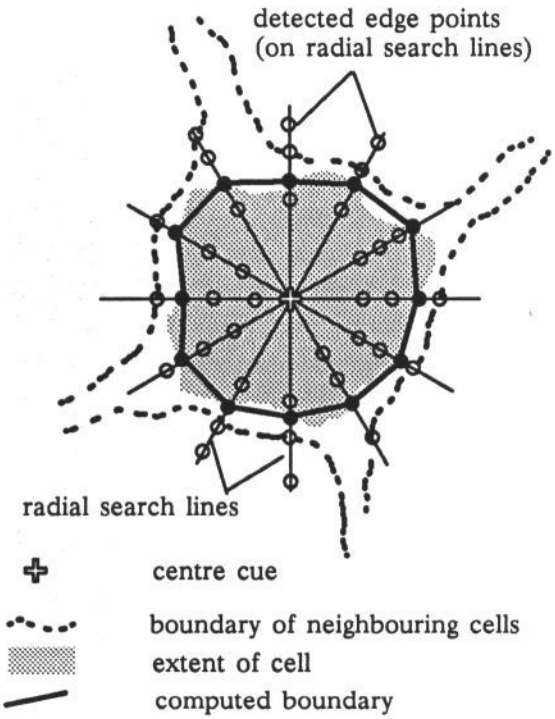

Fig. 6 Boundary search strategy

BOUNDARY INSTANTIATION

The result of boundary cue generation is a table of n ordered sets of m candidate boundary points. The next step is to select the set of points representing the boundary by tracing the appropriate path through the table. The knowledge that the radials are ordered and that the boundary is not re-entrant (see table 1) is used to restrict the problem to the selection of a path which passes through one (and only one) point in each radial set. This is achieved using a dynamic programming algorithm[1 7]. The boundary points are selected on the basis that they are likely to lie on the inside edge of a gap between adjacent fibres and that radial continuity should be preserved as much as possible. These constraints are embodied in a function

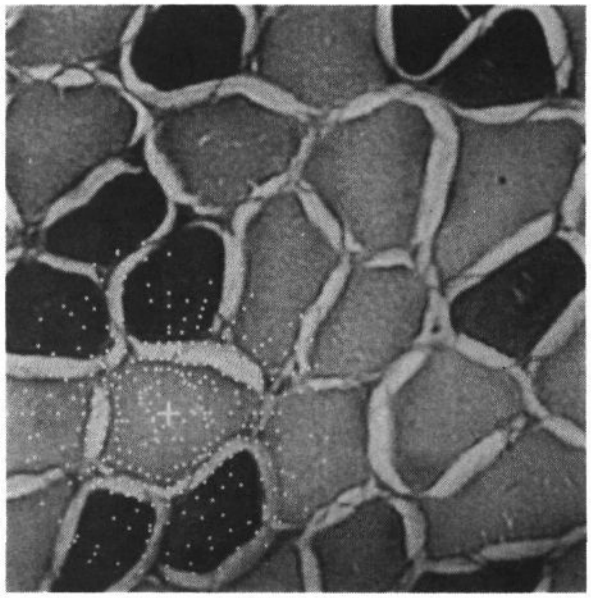

Figure 7. The set of boundary cues for a single fibre.

which assigns a cost to each of the possible pairings of adjacent boundary cues. The dynamic programming algorithm is used to find the path with the globally lowest accumulated cost defined by the cost function. This is taken to represent the set of boundary cues which most closely match the true boundary. The cumulative cost h of a path traced through n points x_1 .. x_n is:-

$$h(x_1..x_n) = a \sum_{k=1}^{n} G(x_k)^{\alpha} + b \sum_{k=2}^{n} R(x_{k-1}, x_k)^{\beta}$$

where a, b, α, β and n *are constants.*

The first term $G(x_k)$, a measure of the significance of the grey-level gap between fibre boundaries is given by:-

$$G(x_k) = \begin{cases} 1 - \sqrt{(|g_i| \times |g_{i+1}|)} & g_i > 0,\ g_{i+1} < 0 \\ 1 & \textit{otherwise} \end{cases}$$

$1 < i < m$, m *is a constant.*

where g_i is the normalised gradient of the edge at boundary cue position i, and the boundary cue positions are numbered sequentially from the centre outwards. Gradient magnitudes along each radial are normalised with respect to the largest gradient on the line. Values greater than zero represent a transition from light to dark in an outwards direction along the radial. Values of less than zero represent a transition in the opposite direction.

The second term $R(x_{k-1}, x_k)$ is a measure of radial continuity and is computed as:-

$R(x_{k-1}, x_k) = (|r_{j,k-1} - r_{i,k}|) \quad 1 \le i \le m;\ 1 \le j \le m$

$r_{i,k}$ is the normalised radial distance of boundary cue i along radial k.

The constants a, b, α and β control the relative importance of the geometric and grey-level edge constraints in the model. The values used for these constants in the experiments we report here were $a=1$,

$b=10$, $\alpha=1$, $\beta=2$. The number of radial search lines (m) was 40 and the number of candidate edge points (n) detected on each radial line was 8. This means that the radial continuity constraint was applied in proportion to the square of the radial distance between sequential candidate boundary points. The value of coefficient b was chosen so that the magnitude of components of the cost function concerned with edge strength and shape were reasonably balanced for typical fibres. The choice of this value was not critical.

The dynamic programming algorithm allows all paths through the ordered radial sets of edge points to be exhaustively searched to find the optimal (lowest cost) path with computational complexity of only $O(nm^2)$. The result for a single boundary is shown in Fig. 8 and the result for a complete field in Fig. 9. It is important to note that the results of boundary instantiation are not sensitive to the location of the centre cues.

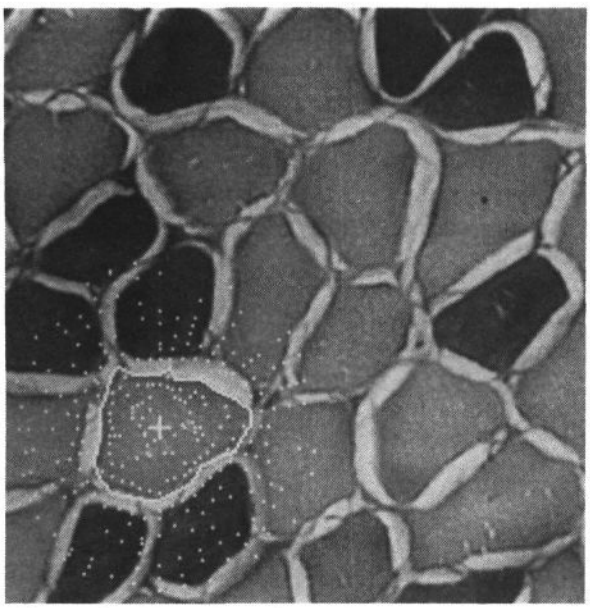

Figure 8. Boundary through selected edge points shown in figure 7.

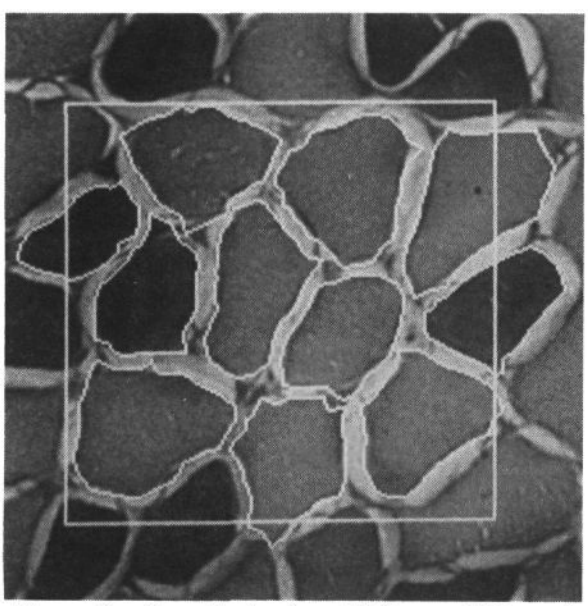

Figure 9. Boundaries for all fibres within region of interest.

IMPLEMENTATION

The results shown were obtained with images digitised to 256 x 256 pixels with 6 bit grey-level resolution. The images were obtained using a standard CCIR TV camera coupled to a light microscope with an objective magnification of x 40.

The software was implemented on both Magiscan 2 (Joyce Loebl) and CVAS 3000 (Visual Machines Ltd) image processing systems and on a SUN 3/160 (SUN Microsystems Ltd) workstation with an IPB 3000 intelligent frame store (Wolfson Image Analysis Unit). The algorithm was coded in a combination of Pascal and frame store microcode in each case. Typical execution times for detecting a single boundary are 35 seconds on a Magiscan 2 and 11 seconds on a CVAS 3000 although it should be noted that no attempt has yet been made to optimise the efficiency of the implementation.

DISCUSSION

We have demonstarted that a strategy combining cue generation with model-based boundary instantiation can achieve results which compare well with those obtained using more complex procedural techniques[3, 5]. The methodology allows robust performance whilst employing relatively simple algorithms. This is demonstrated by the degree of variability in the appearance of the fibres shown in Fig. 9 which have nevertheless been correctly segmented. We have also demonstrated the flexibility of the method by applying it sucessfully to a number of other biological and industrial problems. Fig. 10 shows the result of applying the boundary detection technique (using the same model) to a slit microscope image of corneal endthelial cells.

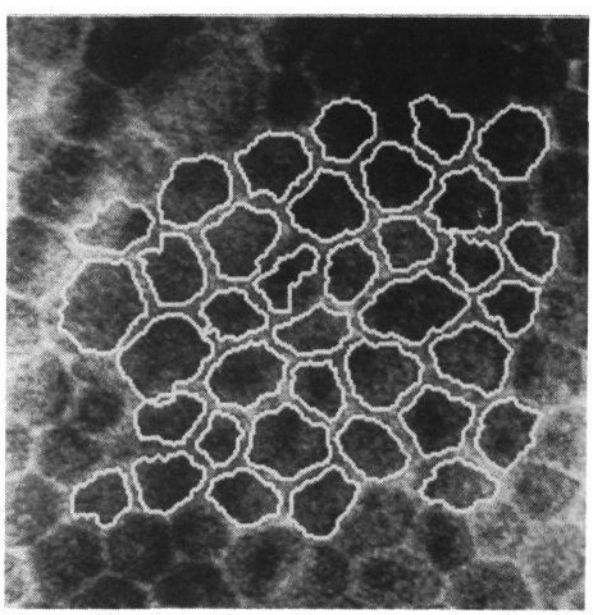

Figure 10. Detection of boundary of endothelial cells in the cornea.

In addition to providing an effective method of collecting, organising and evaluating evidence, our strategy is also computationally efficient. Attention-focussing behaviour ensures that the system concentrates computing power on the collection and evaluation of relevant evidence. The time taken to detect the boundary of a muscle fibre (11 seconds on a CVAS 3000) is similar to the average time per fibre taken by a human being given the task of manually digitising similar boundaries for a large number (>100) of fibres. Considerable improvement should be possible given some attention to the details of implementation.

There are a number of improvements to the method which could easily be made. Immediate requirements include the addition of mechanisms for recovering from errors in the boundary detection process and for 'recognising' fibre boundaries. For example, the gradient of the cumulative cost associated with a particular boundary could be used to focus attention on localised sections which tended to violate, if only to a limited degree, the specification of the model and the total cost associated with a boundary could be used as a figure of merit for the degree of match between the model and its instantiation. The system might then treat all boundaries detected as candidates to be manipulated at a higher level. A model incorporating topographical features of muscle tissue could be used to focus attention on the likeliest interpretation at that level.

Fundemental work is required to develop more general methods of object cue generation, to achieve more explicit knowledge representation and to provide a more sophisticated, trainable scheme of control. These issues are currently being addressed in a separate programme of research which is described elsewhere in these proceedings[4, 11, 12].

REFERENCES

1. **Bellman, R. and Dreyfus, S.** *'Applied Dynamic Programming'* Princeton University Press, Princeton, NJ, (1962).
2. **Borgefors, G.** 'Distance transformations in arbitrary dimensions' *Computer Vision Graphics Image Process.* Vol 27 (1984) pp 321-345.
3. **Castleman, K.R., Chui, L.A., Martin, T.P. & Edgerton, V.R.** 'Quantitative muscle biopsy analysis' in **Greenberg, S.D. (ed)** *'Computer-assisted image analysis cytology'* Karger, Basel, (1984).
4. **Cooper, D., Bryson, N, and Taylor, C.J.** 'An Object Location Strategy using Shape and Grey-level Models' (1988) *Proceedings AVC88.*
5. **Jain, A.K., Smith, S.P. and Backer, E.** 'Segmentation of muscle cell pictures: a preliminary study' *IEEE Trans Pattern Anal Machine Intell.* Vol PAMI-2 (1982) pp 232-242.
6. **Mc Queen, M.P.C.** 'A generalisation of template matching for recognition of real objects' *Pattern Recognition* Vol 13 (1981) pp 139-145.
7. **Montanari, U.** 'On the optimal detection of curves in noisy pictures' *Comm ACM* Vol 14 (1971) pp 335-345.
8. **Rosenfeld, A., Hummel, R. and Zucker, S.W.** 'Scene labeling by relaxation operations' *IEEE Trans. Syst. Man. Cybern.* Vol SMC-6 (1976) pp 420-433.
9. **Serra, J.** *'Image Analysis and Mathematical Morphology'* Academic Press, London, UK (1982).
10. **Taylor, C.J., Graham, J. and Cooper, D.H.** 'System architectures for interactive knowledge-based image-interpretation' *Phil. Trans. R. Soc. Lond.* A 324 (1988) pp 457-465.
11. **Thornham, A., Taylor, C.J. and Cooper, D.H.** 'Object cues for model-based image interpretation' (1988) *Proceedings AVC88.*
12. **Woods, P.W., Pycock, D. and Taylor, C.J.** 'A frame based system for modelling and executing visual tasks' (1988) *Proceedings AVC88.*